

Exclusive diffraction and Pomeron trajectory in ep collisions

S. Fazio^{a,b*} and L. Jenkovszky^{c,d*}

^a *Dipartimento di Fisica, Università della Calabria
Istituto Nazionale di Fisica Nucleare, Gruppo collegato di Cosenza
I-87036 Arcavacata di Rende, Cosenza, Italy*

^b *Joint Institute for Nuclear Research, 141980 - Dubna, Moscow Region, Russia*

^c *Bogolubov Institute for Theoretical Physics, National Academy of Sciences of Ukraine
Kiev-143, 03680 Ukraine*

^d *KFKI, RMKI, Budapest, Hungary*

Abstract

The exclusive diffractive production of vector mesons and real photons in ep collisions has been studied at HERA in a wide kinematic range. Here we present the most recent experimental results together with a Regge-type model. We deduce the Pomanchuk trajectory (Pomeron) by analyzing the HERA data on deeply virtual Compton scattering (DVCS), and then discuss its basic properties, namely its apparent “hardness” and its “non-flat” behavior, different from the claims of some authors.

◊ *e-mail address:* fazio@fis.unical.it

* *e-mail address:* jenk@bitp.kiev.ua

1 Introduction

The diffractive scattering is a process where the colliding particles scatter at very small angles and without any color flux in the final state. This involves a propagator carrying the vacuum quantum numbers, called Pomeron and described, in the soft regime, within the Regge theory. Since the first operation period in 1992, ZEUS and H1, the two experiments dedicated to the DIS physics at HERA, observed that a big amount ($\sim 10\%$) of lepton-proton DIS events had a diffractive origin opening a new area of studies in diffractive production mechanism, providing a hard scale which can be varied over a wide range and therefore it is an ideal testing for QCD models.

In particular, the diffractive production of Vector Mesons (VMs) and real photons in ep collisions allows to study the transition from the soft to the hard regime in strong interactions. The hard regime (high energy and low Bjorken- x) is dominated by the exchange of a hard Pomeron sensitive to the gluon content and well described by perturbative QCD (pQCD), while in the soft regime (low- x) the interaction is well described within the Regge phenomenology. Indicating with Q^2 the virtuality of the exchanged photon and with M^2 the square mass of the produced VM, HERA data suggested a universal hard scale, $Q^2 + M^2$, for the diffractive exclusive production of VMs and real photons, which indicates the transition from the soft to the hard regime.

2 Q^2 and W dependence of the cross section

A new precision measurement of the reaction $\gamma^*p \rightarrow \rho^0p$ was published by ZEUS [1]. It was found that the cross section falls steeply with the increasing of Q^2 but, unlike it was

observed for the J/ψ electroproduction [2, 3], it cannot be described by a simple propagator term like $\sigma \propto (Q^2 + M^2)^{-n}$, in particular an n value increasing with Q^2 appears to be favored. Figure 1 reports the cross section for the ρ^0 electroproduction versus Q^2 compared with several theoretical predictions: the KWM model [4] based on the saturation model, the FSS model [5] with and without saturation and the DF model [6]. None of the available models gives a good description of the data over the full kinematic range of the measurement.

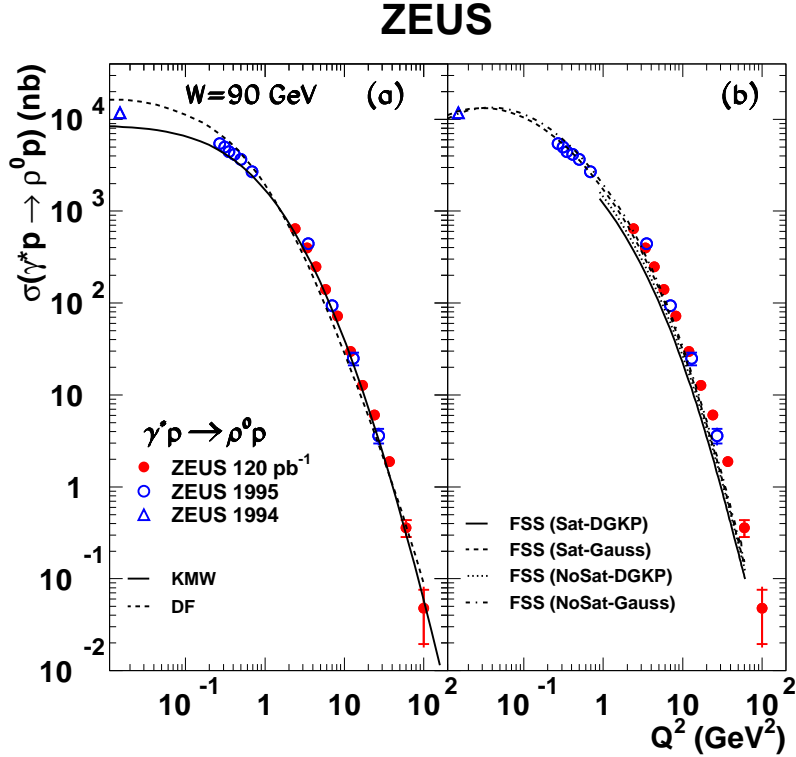


Figure 1: The $\gamma^*p \rightarrow \rho^0 p$ cross section as a function of Q^2 measured at $W = 90 \text{ GeV}^2$ and compared in (a) and (b) with different models as described in the text.

The soft to hard transition can be observed looking at the dependence of the VMs photoproduction ($Q^2 = 0$) cross section from the γ^*p centre of mass energy, W , where the scale is provided by M^2 . Figure 2 collects the $\sigma(\gamma^*p \rightarrow Vp)$ as a function of W from the lightest vector meson, ρ^0 , to the heaviest, Υ , compared to the total cross section. The cross section rises with the energy as W^δ , where the δ exponent increases with the hard scale M^2 as expected for a transition from the soft to the hard regime. New results on the Υ photoproduction [7], recently published by ZEUS, confirmed the steeper rise of $\sigma(W)$ for higher vector meson masses.

The transition from the soft to the hard regime can also be studied varying Q^2 . Recent results were achieved by H1 [?] and ZEUS [9] for the exclusive production of a real photon, the Deeply Virtual Compton Scattering (DVCS), where the hard scale is provided only by the photon virtuality, Q^2 . Figure 3 shows the H1 (left) and the ZEUS (right) results. The steep rise with W of the cross section even at low- Q^2 , seems to suggest that the most sensitive part to the soft scale comes from the wave function of the produced VM. A similar result was obtained for the J/ψ electroproduction [2, 3].

The electroproduction of a large variety of VMs was studied at different Q^2 values and

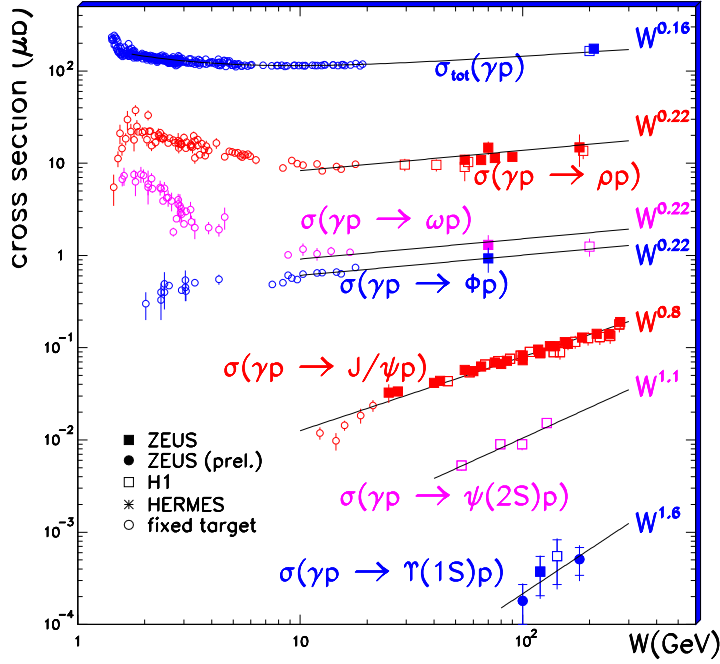


Figure 2: The W dependence of the cross section for exclusive VM photoproduction together with the total photoproduction cross section. Lines are the result of a W^δ fit to the data at high W -energy values.

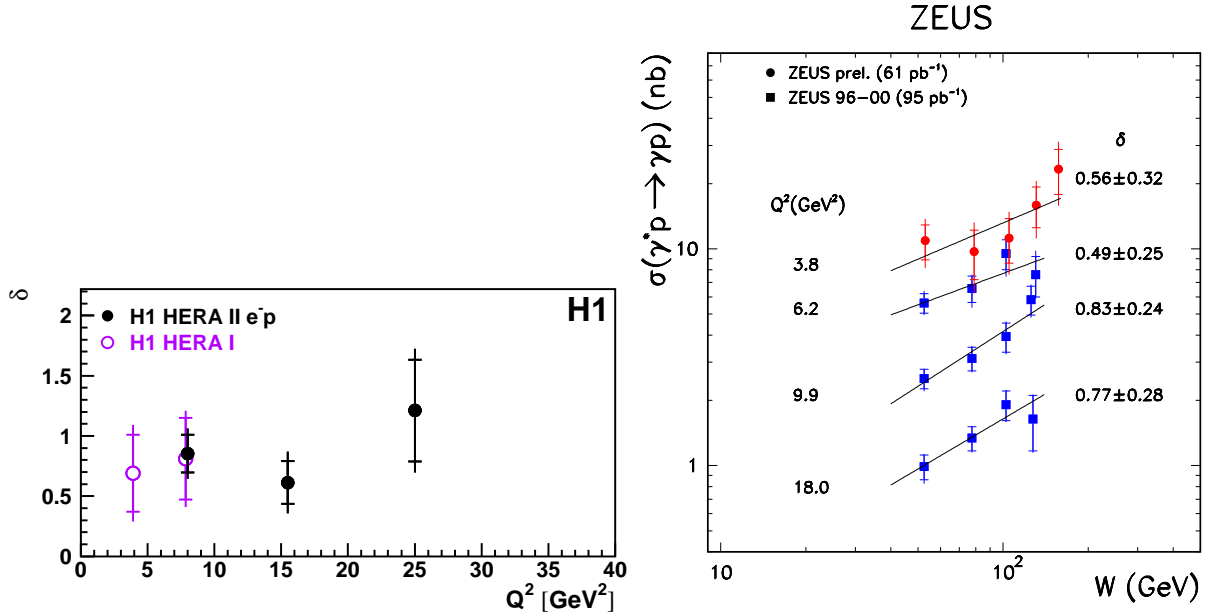


Figure 3: The W dependence of the cross section for a DVCS process. Lines come from a W^δ fit to the data. Left: the H1 measurement of the δ slope as a function of Q^2 . Right: the new ZEUS preliminary measurement at low Q^2 (dots) together with the published measurements (squares).

the corresponding slope δ is reported in Fig. 4 (left) versus the scale $Q^2 + M^2$, including the DVCS measurements. Data show a logarithmic shape $\delta \propto \ln(Q^2 + M^2)$ and the behaviour seems to be universal with δ increasing from 0.2 at low scale, as expected from a soft Pomeron exchange [10] to ~ 0.8 at large scale values.

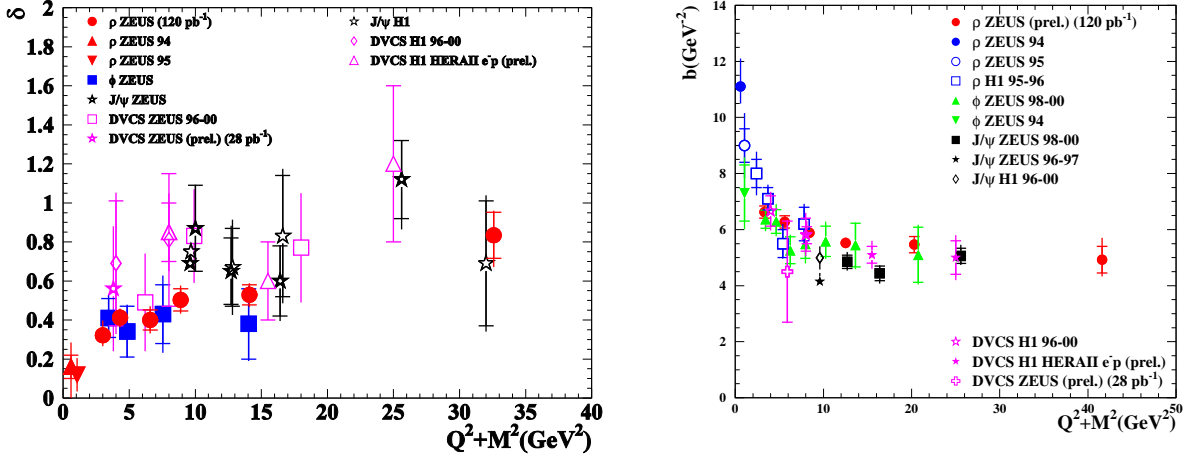


Figure 4: The dependence on the hard scale $Q^2 + M^2$ of the value δ (left) extracted from a fit W^δ and of the slope B (b in the figure label) (right) extracted from a fit $\frac{d\sigma}{dt} \propto e^{B|t|}$ for the exclusive VM electroproduction. DVCS is also included.

3 t dependence of the cross section

The differential cross section as a function of t , the four-momentum transfer at the proton vertex, can be parametrised by an exponential fit: $\frac{d\sigma}{d|t|} \propto e^{B|t|}$. Figure 4 (right) reports the collection of the B values versus the scale $Q^2 + M^2$ for the electroproduction of VMs and DVCS, with B decreasing from $\sim 11 \text{ GeV}^{-2}$ to $\sim 5 \text{ GeV}^{-2}$ as expected in hard regime.

The measurement of $d\sigma/d|t|$ for the DVCS process, recently published by the H1 Col- lab [?], where t was obtained from the transverse momentum distribution of the photon, studied B versus Q^2 and W as shown in Fig. 5. B seems to decrease with Q^2 up to the value expected for a hard process but it doesn't depend on W . A new preliminary

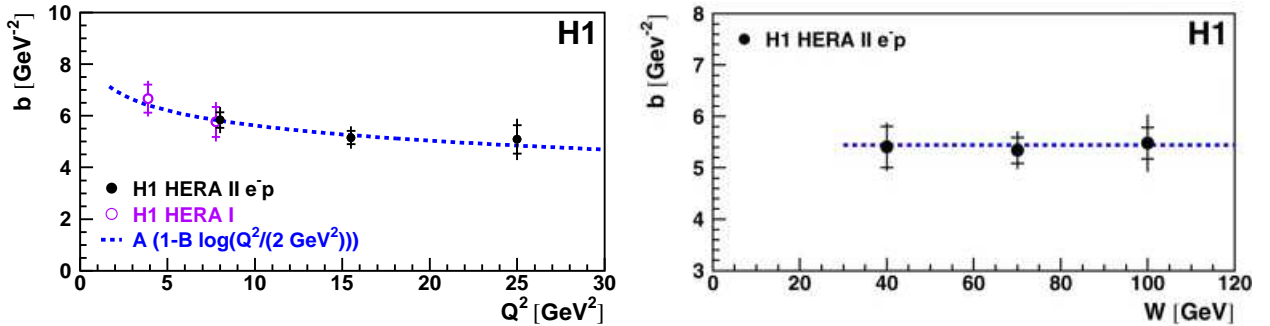


Figure 5: The t slope parameter B (b in the figure label) as a function of Q^2 (left) and W (right).

ZEUS measurement [9] of $d\sigma/d|t|$ has been achieved from a direct measurement of the proton final state of using a spectrometer based on the roman pot technique. The result $B = 4.4 \pm 1.3$ (*stat.*) ± 0.4 (*syst.*) GeV^{-2} , measured at $Q^2 = 5.2 GeV^2$ and $W = 104 GeV$, is consistent, within the large uncertainties due to the low acceptance of the spectrometer, with the H1 result [?] of $B = 5.45 \pm 0.19$ (*stat.*) ± 0.34 (*syst.*) GeV^{-2} at $Q^2 = 8 GeV^2$ and $W = 82 GeV$.

Since the B value can be related via a Fourier transform to the impact parameter and assuming that the exclusive process in the hard regime is dominated by gluons, the relation $\langle r^2 \rangle = 2b(\hbar c)^2$ can be used to obtain the radius of the gluon confinement area in the proton. $b \sim 5 GeV^2$ corresponds to $\langle r^2 \rangle \sim 0.6 fm$ smaller than the proton radius ($\sim 0.8 fm$) indicating that the gluons are well contained within the charge-radius of the proton.

4 The Pomeron in DVCS at HERA

Exclusive production of vector states (real photon, VMs, lepton pairs) via deeply virtual scattering, $ep \rightarrow epV$, is interesting for many reasons, above all as a source in extracting informations about General Parton Distributions (GPDs). Of particular interest is DVCS in which the outgoing real photon, interfering with the photon coming from bremsstrahlung (Bethe-Heitler process), offers a holographic picture of the nucleon.

A Q^2 -dependence of generalized parton distributions (GPD) can be found from QCD evolution, similar, although less explored than that of ordinary parton distribution, obeying the DGLAP evolution equation ¹.

In the present paper, we analyze and test an explicit model for DVCS. The model can be used to infer the GPD by a relevant deconvolution procedure.

After the shut-down of the electron-proton collider HERA, the H1 and ZEUS collaborations have left a huge heritage of data still waiting for a better understanding. In particular, it concerns the properties of the Pomeron trajectory as seen in VM electroproduction, $ep \rightarrow eVp$, and in DVCS, $ep \rightarrow e\gamma p$. There are many papers discussing in details the form and the values of the parameters of the Pomeron trajectory as well as their possible Q^2 dependence (for recent reviews see, e.g. [11]). In general they introduce a linear Regge-trajectory of the Pomeron

$$\alpha_P(t, Q^2) = \alpha_0(Q^2) + \alpha'(Q^2)t, \quad (1)$$

where t is the squared four-momentum transferred at the proton vertex and Q^2 is the virtuality of the exchanged photon. For the “effective” Pomeron they use the standard Regge pole parametrization of the scattering amplitude

$$A(s, t, Q^2) = A_0 e^{B(t, Q^2)} \left(\frac{s}{1 GeV^2} \right)^{\alpha_P(t, Q^2)}, \quad (2)$$

where $s = W^2$ is the squared γ^*p centre-of-mass energy and $B(t, Q^2)$ is related to the radius associated with the proton vertex.

The problem of constructing Regge-type models for currents (lepton-hadron scattering) or the off-mass-shell continuation of the analytic S -matrix has already a long history, still lacking a consistent solution. The concepts of the analytic S -matrix formally may even be incompatible with, or inapplicable to processes like Compton scattering. Nevertheless, the need for a theoretical framework to describe high-energy lepton-hadron scattering served

¹for a discussion of GPD evolution see the Appendix

as an “excuse” in using Q^2 -dependent Regge-type models for small x (large $s \sim Q^2/x$) processes, like Compton scattering. Moreover, to meet the apparent acceleration of the rise of the structure functions with $1/x$ towards larger Q^2 , a Q^2 dependent Pomeron was introduced, in complete discords with Regge factorization, in which the dependence on the mass or virtuality of the external particle (photon or meson in our case) can enter at most through the relevant vertex function. This inconsistency was circumvented by calling this object “effective Pomeron” (or, more generally, a Reggeon), implying that it accommodates by more than a single Regge exchange, without specifying the content. Very often, however, this was ignored and the parameters of the Pomeron have been extracted from simple formula like in Eq. 1. Most of the conclusions, especially the appearance a large and ever increasing intercept (hard Pomeron) and its small slope (flat Pomeron) were used to confirm perturbative QCD.

At the same time, it was shown [12] that the inclusion of a sub-leading Regge contribution modifies the parameters of the Pomeron, in particular the observed rise of the structure function partly is due to the decrease of the sub-leading contribution, and the Q^2 dependent residue functions can provide for the apparent “hardening” of the Pomeron.

Recently a number of Regge/Pomeron-type models for DVCS appeared in the literature [13, 15, 16, 17].

In the present paper, we analyze the high-energy data on DVCS collected by the H1 and ZEUS detectors at HERA [8, 9, 18, 19]. To do so, we use a model for the Pomeron elaborated and fitted to the data in Ref. [13].

In most of the Regge/pole models used in analyzing the experimental data, a linear Pomeron trajectory is used. Although linear trajectories contradict to the postural of the S -matrix (analyticity and unitarity), to perturbative QCD calculations (BFKL) [14], as well as disagree with precise fits to the data, they can serve as a simple approximation to the observed phenomena at small $|t|$ [13] however the linear behavior is replaced by a logarithmic one ².

For this reason we use a simple Regge pole model for the Pomeron, however, contrary to most of the known models, our Pomeron trajectory is essentially nonlinear.

The scattering amplitude has the form

$$A(s, t, Q^2)_{\gamma^* p \rightarrow \gamma p} = -A_0 e^{b\alpha(t)} e^{b\beta(z)} (-is/s_0)^{\alpha(t)} = -A_0 e^{(b+L)\alpha(t)+b\beta(z)}, \quad (3)$$

where $L \equiv \ln(-is/s_0)$. The trajectory at the $pIPp$ vertex is

$$\alpha(t) = \alpha_0 - \alpha_1 \ln(1 - \alpha_2 t). \quad (4)$$

whereas the trajectory at the $\gamma^*IP\gamma$ vertex is

$$\beta(z) = \alpha_0 - \alpha_1 \ln(1 - \alpha_2 z), \quad (5)$$

with $z = t - Q^2$ - a new variable introduced in Ref. [13]. Notice that the presence of the “minus” sign in Eq. 3 is important for the linear forms, e.g. $ImA(t=0)$, proportional to the total cross section, or for the ratio $\rho = ReA/ImA$, but it is irrelevant for the squared modulus we are interested in.

Similar to [15], we consider only the helicity conserving amplitude. For not too large Q^2 the contribution from longitudinal photons is small (it vanishes for $Q^2 = 0$). Moreover, at the high energies typical of the HERA collider, the amplitude is dominated by the helicity conserving Pomeron exchange and, since the final photon is real and transverse, the initial

²For further arguments see the Ref. [13]

one is also transverse and the helicity is conserved. The electroproduction of vector mesons requires the account for both the longitudinal and transverse cross sections.

Generally speaking, any DVCS reaction admits the contribution from a subleading Regge exchanges, most important of which is the f trajectory, made of a quark and an antiquark, not gluons like the Pomeron. It differs only by the values of the Regge-trajectory parameters (lower intercept and steeper slope).

The cross section can be calculated as

$$\frac{d\sigma}{dt}(s, t, Q^2) = \frac{\pi}{s^2} |A(s, t, Q^2)|^2. \quad (6)$$

with the slope of the $d\sigma/d|t|$ cross section coming from

$$B = \frac{d}{dt} \ln\left(\frac{d\sigma}{dt}\right). \quad (7)$$

The model contains quite a number of parameters but some of them (s_0 , α_1 , α_2) can be fixed by theoretical constraints, as explained in Ref. [13]. Fits to the DVCS data collected at HERA [18, 8, 19] were performed and the results are shown in Fig. 8, with the values of the fit parameters, A_0 , b , α_0 quoted in Table 8. Note that $\sigma(W)$ is sensitive to the Pomeron intercept, α_0 , and the corresponding fit was performed by keeping $b_P = b = 1.0$ fixed, while the $\sigma(Q^2)$ is sensitive to b and the corresponding fit was done at fixed $\alpha_0 = 1.2$. Figures 6a,b show that the model can reproduce all the features of data versus Q^2 and $W = \sqrt{s}$. Results suggest that the Pomeron in DVCS has an intercept, $\alpha_0 \simeq 1.2$ greater than that in hadronic reactions, but a slope, $\alpha' \simeq 0.25$, typical of hadronic scattering and not so flat as it was observed for the diffractive electroproduction of vector mesons ($\alpha' \sim 0.1 \simeq 0.5\alpha_h h'$) in hard regime.

Parameter	σ_{DVCS} vs Q^2	σ_{DVCS} vs W	$d\sigma/d t $ H1	$d\sigma/d t $ ZEUS
A_0	0.13 ± 0.01	0.10 ± 0.01	0.17 ± 0.01	0.44 ± 0.10
α_0	fixed at 1.2	1.23 ± 0.006	fixed at 1.2	fixed at 1.2
b	0.96 ± 0.07	fixed at 1.0	fixed at 1.0	fixed at 1.0
$\tilde{\chi}^2$	1.39	1.21	16.8	0.3

Table 1: Values of fitted parameters and the correspondent $\tilde{\chi}^2$ value.

The fit of $d\sigma/d|t|$ was performed with all the parameters fixed excepted for the normalisation. The model does not agree with the H1 measurements (see Fig. 6c) but it is compatible with the new ZEUS preliminary results (see Fig. 6d). The t variable was calculated in H1 by the transverse four-momenta of the scattered electron and the real photon, using the approximation $t \simeq |P_{T_e} + P_{T_\gamma}|^2$, while in ZEUS a particular silicon microstrips spectrometer, based on the roman pots technique, was used in order to have a direct measurement of the scattered proton momentum \vec{p}' and then t being calculated from the quantity: $x_L = \frac{p'_z}{p_{beam}}$, by the phormula: $t = \frac{p_x'^2 + p_y'^2}{x_L} + E_{beam}^2 \frac{(x_L - 1)^2}{x_L}$. The really low acceptance of this spectrometer is the reason of the poor statistics of the ZEUS data, however it offers a really pure selection of diffractive events, not affected by any not-diffractive background. The agreement with the ZEUS preliminary measurements encourages us to be still confident in our predictions, till they will be checked by the new HERA data analyses (now in progress with and without roman pots spectrometer).

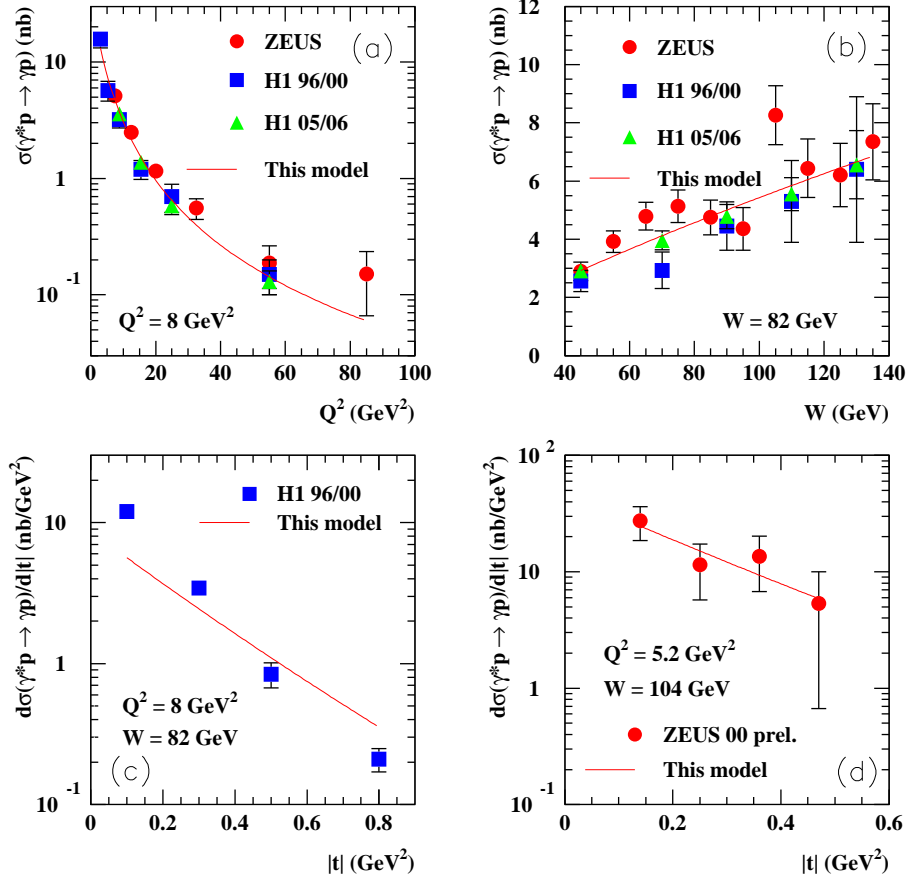


Figure 6: Upper panel: Energy (a) and Q^2 (b) dependence of the DVCS cross section, the model is fitted to the HERA data. Lower panel: the prediction for the t dependence of the cross section is compared with H1 (c) and ZEUS (d) data with only the normalisation kept as a free fit parameter. Error bars include both statistical and systematic uncertainties summed in quadrature. The error bars include both the statistical and systematic uncertainties summed in quadrature.

The slope of $d\sigma/d|t|$, calculated according to Eq. 7, is depicted in Fig. 7 as a function of Q^2 and W and is compared with de HERA measurements. The local slope is predicted to slightly rise with W but to be almost independent on Q^2 .

Eq. 7 was then used to make a collection of figures showing the slope dependence for different values of W and t . The t dependence of the local slope calculated from Eq. 7 is shown in Fig. 8a at fixed $Q^2 = 4$ GeV² for three different values of energy.

Figure 8b depicts the Q^2 dependence of the local slope at $W = 60$ GeV for several values of t .

Figure 8c shows the energy dependence of the local slope at $Q^2 = 4$ GeV² for several values of t .

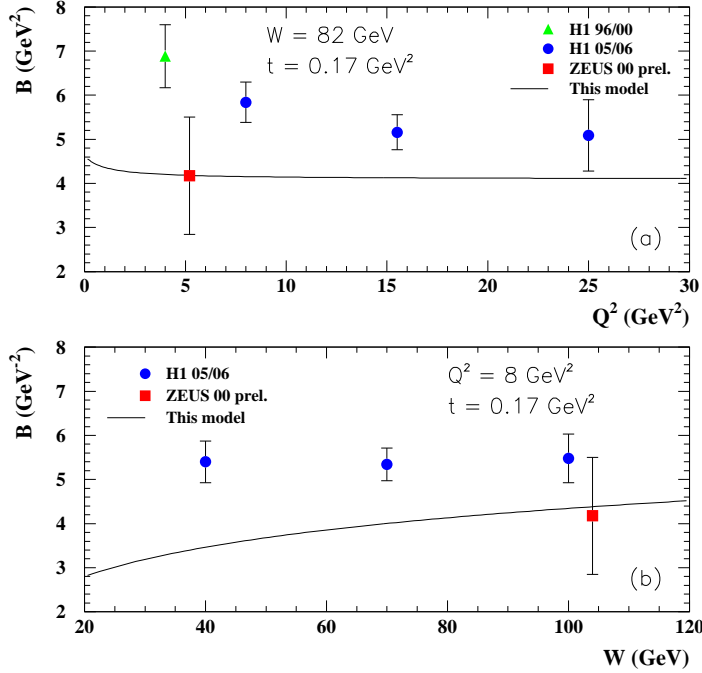


Figure 7: *Slope of the cross section vs Q^2 and W as calculated from Eq. 7, compared with the HERA data.*

5 Conclusions

- After the shut-down of the HERA Collider, the ZEUS and H1 experiments have left a huge heritage of experimental results on the diffractive production of vector mesons and real photons still waiting for a better understanding. Nevertheless, new analyses on HERA data are still in progress.
- We show that data on DVCS from HERA can be fitted with a semi-hard Pomeron, not being flat.
- The Pomeron trajectory could be a non-linear function; it is nearly linear at small and moderate values of $|t|$, leveling off at large $|t|$. The same logarithmic trajectory could be used in hadronic reactions, for example in analyzing, with higher precision, the future diffractive exclusive data from LHC, where details, such as the two-pion threshold [32], neglected here, should be taken into account.
- Here we used a simple “minimal” model, with a small number of the free parameters, which, in view of the limited number of data points, made possible the convergence of the minimization procedure. A more detailed analysis should include also the individual contributions from the longitudinal and transverse cross sections, though their ratio R , spin effects, reaction ratios and comparison with possible QCD predictions, especially concerning the evolution in Q^2 (see next item and Appendix).
- A complete solution for the Q^2 evolution in DVCS has not been yet found, although partial results are known from the literature. In a simplified, pragmatic approach the

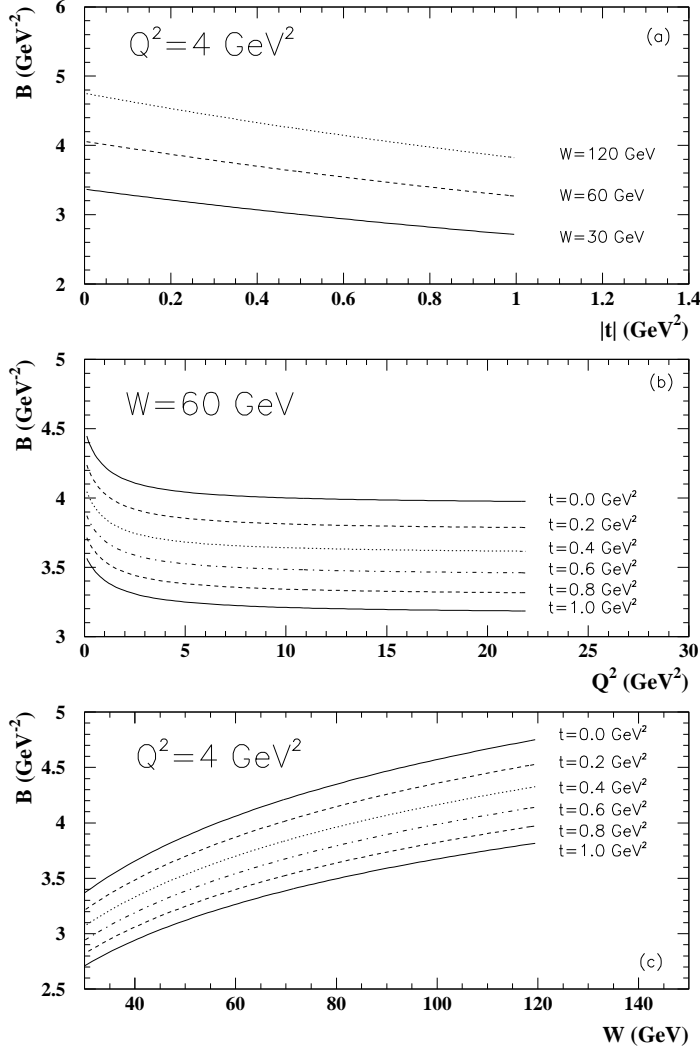


Figure 8: *Slope of the cross section as calculated from Eq. 6. for several values of W , Q^2 and t .*

Q^2 and t dependence in a DVCS (actually not factorizable!), reduces the problem to the evolution of ordinary DIS by the DGLAP procedure. These attempts are summarized in Appendix.

- The model and the fitting procedure presented in this paper can be extended to high-energy vector meson production. We intend to do so in a forthcoming publication. Let us notice also that any consistent extension/interpolation of the Regge approach to low energies (resonance region) should involve dual models, as it was shown [33] for the Pomeron component in case of J/Ψ scattering.

Acknowledgment We would like to thank R. Fiore, F. Paccanoni and V. Nikitin for the helpful discussions. L. Jenkovszky thanks the University of Calabria, where part of this work was done, for its hospitality and support.

APPENDIX. GPD and QCD evolution of DVCS

From Eq. 3 we get the real and imaginary parts of the DVCS amplitude at $Q^2 = Q_0^2$, that will be useful for the evolution:

$$ImA_{DVCS}(x_{Bj}, t, Q_0^2) = \sin[\pi\alpha(t)/2]G(t, Q_0^2)\left(\frac{Q_0^2}{s_0x_{Bj}}\right)^{\alpha(t)}, \quad (8)$$

$$ReA_{DVCS}(x_{Bj}, t, Q_0^2) = -\cos[\pi\alpha(t)/2]G(t, Q_0^2)\left(\frac{Q_0^2}{s_0x_{Bj}}\right)^{\alpha(t)}, \quad (9)$$

where

$$G(t) = e^{b[\alpha(t)+\beta(t, Q_0^2)]}. \quad (10)$$

Skewendess is defined in terms of the Bjorken variable x_{Bj} as $\xi \simeq 2x_{Bj} - x_{Bj}$ and v.v., $x_{Bj} \simeq 2\xi/(1 + \xi)$.

The aim is to evolve this amplitude to higher values of Q^2 , $Q^2 > Q_0^2 \sim 1\text{Gev}^2$ and, at the same time, to grasp the most important properties of the corresponding generalized parton distributions (GPD).

The singlet combination of GPD, corresponding to the exchange in the t - channel of a $C = +1$ charge conjugation, even signature reggeon is [27]

$$H^{q(+)}(x, \xi, t) = H^q(x, \xi, t) - H^q(-x, \xi, t), \quad (11)$$

with $H^{q(+)}(x, 0, 0) = q(x) + \bar{q}(x)$, where $q(x)$ is the usual quark distribution for quark q . Its evolution is well known. The ‘‘valence’’ combination, odd signature, is even under the change: $x \rightarrow -x$.

The point $x = \xi$, where DGLAP ($|x| > \xi$) [21] and ERBL ($|x| < \xi$) [22] regimes meet, is directly accessible to experiment since, at leading order in α_s , the imaginary amplitude part of the amplitude A for DVCS is proportional to a GPD at $x = \xi$ [23]

$$ImA_{DVCS}(x_{Bj}, t, Q_0^2) = -\pi \sum_q e_q^2 H^{q(+)}(\xi, \xi, t, Q_0^2), \quad (12)$$

where $H^{q(+)}(\xi, \xi, t, Q_0^2)$ is known from Eq. 8. Unfortunately, the evolution equation for $H^{q(+)}(\xi, \xi, t, Q_0^2)$ involves $H^{q(+)}(x, \xi, t, Q_0^2)$ for x in the interval $[0, 1]$ (for DVCS), to be known.

An approximate solution based on conformal invariance, valid at one loop level is possible [24]. The off-forward matrix elements of a set of twist-two operators, whose leading-log evolution is diagonal due to conformal symmetry, are the Gegenbauer polynomials. In the forward kinematics, the Gegenbauer polynomials reduce to polynomials in x_{Bj} . In Ref. [25] an explicit transformation has been constructed relating the off-forward and the forward evolutions.

Usually it is very difficult to apply the transformation constructed in Ref. [25] to a realistic problem but, in our case, the simplicity of the input at Q_0^2 makes possible an explicit asymptotic solution for small ξ_{Bj} and $\xi \sim x_{Bj}/2$. It has been shown in Ref. [26] that, in the phenomenologically important small- ξ and $|t|$ region, the off-diagonal distributions are determined unambiguously by the small- x behavior of the diagonal parton distributions. By setting

$$H(x, \xi) \equiv H(x, \xi, t, \mu^2), \quad (-1 \leq x_{Bj} \leq 1), \quad (13)$$

where the values of t and ξ do not change in the evolution to a higher scale μ^2 , it was shown in Ref. [26] that at small ξ

$$H^q(x, \xi) = \int_{-1}^1 dx' \left[\frac{2}{\pi} \Im \int_0^1 \frac{ds}{y(s) \sqrt{1 - y(s)x'}} \right] \frac{d}{dx'} \left(\frac{q(x')}{|x'|} \right), \quad (14)$$

$$y(s) = \frac{4s(1-s)}{x + \xi(1-2s)}. \quad (15)$$

The proof of Eq. 14 uses the properties of the diagonal parton distributions

$$q(x' \rightarrow 1) \rightarrow 0, \quad q^s(x') = -q^s(-x'), \quad q^{ns}(x') = q^{ns}(-x'),$$

that corresponds to the symmetry relations

$$H^i(x, \xi) = H^i(x, -\xi), \quad (i = (q, w), (q, ns),$$

$$H^{q,s}(x, \xi) = H^{q,s}(-x, \xi),$$

$$H^{q,ns}(x, \xi) = H^{q,ns}(-x, \xi),$$

where, as usual, s stays for “singlet” quark contribution and n_s means “non-singlet”. At small ξ , the same anomalous dimensions γ_N control both the diagonal and off-diagonal evolution.

Consider now the prediction of [26] for the off-diagonal distribution $H^q(x, \xi)$ by making the physically reasonable small- x assumption that

$$xq(x) = N_q x^{-\lambda_q}, \quad (16)$$

where λ_q may depend also on t , $\lambda_q = \lambda_q(t)$. Then eq. (18) can be integrated

$$H^q(x, \xi) = N_q \frac{\Gamma(\lambda + 5/2)}{\Gamma(\lambda + 2)} \frac{2}{\sqrt{\pi}} \int_0^1 ds \left[\frac{4s(1-s)}{x + \xi(1-2s)} \right]^{\lambda_q + 1}, \quad (17)$$

where, for singlet quarks (i.e. when $\lambda_q < 1$) the integral is a principal value integral and Eq. 17 becomes integrable for any $\lambda_q < 1$.

The distribution $H^q(x, \xi)$, for small ξ , has the form [26]

$$H^q(x, \xi) = \xi^{-\lambda_q - 1} F_q(x/\xi)$$

with

$$H^q(\xi, xi) = \xi^{-\lambda_q - 1} F_q(1),$$

where $F_q(z)$ is a function determined by Eq. 17. Similarly, if $xg(x) = N_g x^{-\lambda_g}$, then $H^q(\xi, \xi) = \xi^{-\lambda_g} F_g(1)$ at small ξ . Viceversa, since the amplitude in Eqs. 8, and 9 is of Regge form and is proportional to $\xi^{-\alpha(t)}$ for small ξ and fixed Q^2 , then

$$\sum_q e_q^2 H(\xi, \xi) = -\frac{1}{\pi} \text{Im} A_{DVCS} \propto \xi^{-\alpha(t)} \quad (18)$$

and the parton distribution that appears in Eq. 14 has the form

$$xq(x) \propto x^{-\alpha(t)+1}, \quad (19)$$

where $xq(x)$ can represent $F_2(x)$ if we start from Eq. 18.

An approximate analytic evolution of the input singlet parton distribution is well known if the input is of the Regge-like form. Since only the diagonal parton distributions are involved in the calculations, one can resort to libraries that generate parton distributions but, since we are interested in the small- ξ region. Equation 14 then determines the Q^2 dependence of $H^q(x, \xi)$ and, finally, Eq. 18 gives the scale dependence of ImA_{DVCS} . The knowledge of $H^{q(+)}(x, \xi)$ fixes also, at leading order in α , since

$$A_{DVCS}(\xi, t, Q^2) = \sum_q e_q^2 \int_0^1 H^{q(+)}(x, \xi, t, Q^2) \left(\frac{1}{x - \xi + i0} + \frac{1}{x + \xi - i0} \right). \quad (20)$$

Similar results were obtained in a recent paper [27].

References

- [1] ZEUS Coll., S.Chekanov et al., *PMC Phys. A*, 1 (2007).
- [2] ZEUS Coll., S.Chekanov et al., *Nuc. Phys. B* **695**, 3 (2004).
- [3] H1 Coll., S.Chekanov et al., *Eur. Phys. J. C* **46**, 585 (2006).
- [4] H. Kowalski, L. Motyka and G. Watt, *Phys. Rev. D* **74**, 074016 (2006).
- [5] J.R. Forshaw, R. Sandapen and G. Shaw, *Phys. Rev. D* **69**, 094013 (2004).
- [6] H.G. Dosch and E. Ferreira, *Eur. Phys. J. C* **51**, 83 (2007).
- [7] ZEUS Coll., S.Chekanov et al., *ZEUS-prel-07-015*.
- [8] H1 Coll., F.D. Aaron et al., *Phys. Lett. B* **659**, 796 (2008).
- [9] ZEUS Coll., S. Chekanov et al., Presented at the EPS07 Conference, 19-25 July 2007, Manchester (England), *ZEUS-prel-07-016*.
- [10] A. Donnachie and P.V. Landshoff, *Phys. Lett. B* **296**, 227 (1992).
- [11] Aharon Levy, for the ZEUS collaboration, arXiv:0706.1867.
- [12] L. Jenkovszky, K. Kontros, A. Lengyel, F. Paccanoni, *Phys. Lett. B* **459** (1999) 265.
- [13] M. Capua, S. Fazio, R. Fiore, L. Jenkovszky, and F. Paccanoni, *Phys. Lett. B* **645** (2007) 161.
- [14] V. S. Fadin, E. A. Kuraev, L. N. Lipatov, *Phys. Lett. B* **60** (1975) 50;
I. I. Balitsky, L. N. Lipatov, *Yad. Fiz.* **28** (1978) 822.
- [15] D. Muller, arXiv:hep-ph/0605013.
- [16] Kresimir Kumericki, Dieter Mueller, Kornelija Passek-Kumericki, *Sum rules and dualities for generalized parton distributions: Is there a holographic principle?*, arXiv:0805.0152.

- [17] F. M. Dittes, D. Mueller, D. Robaschik, B. Geyer and J. Horejsi, Phys. Lett. B **209** (1988) 325;
D. Mueller, D. Robaschik, B. Geyer, F. M. Dittes and J. Horejsi, Fortsch. Phys. **42** (1994) 101.
- [18] H1 Coll., A. Aktas et al., Eur. Phys. J. C **44** (2005) 1.
- [19] ZEUS Coll., S. Chekanov et al., Phys. Lett. B **573** (2003) 46.
- [20] A. Freund, M. McDermott, M. Strikman, Phys. Rev. D **67** (2003) 036001;
L. Favart, M. V. T. Machado, Eur. Phys. J. C **19** (2003) 365;
V. Guzey, M. V. Polyakov, Eur. Phys. J. C **46** (2006) 151.
- [21] V. N. Gribov and L. N. Lipatov, Sov. J. Nucl. Phys. **15** (1972) 48;
L. N. Lipatov, Sov. J. Nucl. Phys. **20** (1975) 94;
G. Altarelli and G. Parisi, Nucl. Phys. B **126** (1977) 298;
Y. L. Dokshitzer, Dov. Phys. JETP **46** (1977) 641.
- [22] A. V. Efremov and A. V. Radyushkin, Phys. Lett. B **94** (1980) 245;
G. P. Lepage and S. J. Brodsky, Phys. Lett. B **87** (1979) 359.
- [23] L. L. Jenkovszky and V. K. Magas, In the Proc. of the XXXI-th ISMD, held in Datong (China), hep-ph/0111398;
R. Fiore, L. L. Jenkovszky and V. K. Magas, ISMD Conference in Rohnert Park (California, USA), Acta Phys. Pol. B **36** (2005) 743.
- [24] T. Orhendorf, Nucl. Phys. B **198** (1982) 26;
A. P. Bukhvostov *et al.* Nucl. Phys. B **258** (1985) 601.
- [25] A. Shuvaev, Phys. Rev. D **60** (1999) 116005.
- [26] A. G. Shuvaev *et al.*, Phys. Rev. D **60** (1999) 014015.
- [27] M. Dihel and W. Kugler, hep-ph/0711.2184.
- [28] V. N. Gribov, L. N. Lipatov, Sov. J. Nucl. Phys. **15** (1972) 438 and 675;
G. Alterelli and G. Parisi, Nucl. Phys. B **126** (1977) 298.
- [29] V. Guzey and M. V. Polyakov, hep-ph/0507183.
- [30] M. Kirch, A. Manashov, A. Schafer, Phys. Rev. D **72** (2005) 114006.
- [31] A. V. Vinnikov, hep-ph/0604248.
- [32] G. Cohen-Tannoudji et al., Lettere NC, **5** (1972) 957.
- [33] L. L. Jenkovszky, R. Fiore, V. K. Magas, F. Paccanoni and A. Prokudin, Phys. Rev. D **75** (2007) 116005.